Int. J. Heat Mass Transfer. Vol. 29, No. 1, pp. 119–133, 1986
Printed in Great Britain

0017–9310/86 $3.000.00

Natural convection heat transfer from a horizontal cylinder embedded in a porous medium

R. M. FAND, T. E. STEINBERGER and P. CHENG
Department of Mechanical Engineering, University of Hawaii at Manoa, Honolulu, HI 96822, U.S.A.

(*Received* 29 *April* 1985 *and in final form* 22 *July* 1985)

Abstract—This paper presents the results of an experimental investigation of heat transfer by natural convection from a horizontal cylinder embedded in porous media consisting of randomly packed glass spheres saturated by either water or silicone oil. It is shown that the overall range of the Rayleigh number, Ra, can be divided into two subregions, called 'low' and 'high', in each of which the Nusselt number, Nu, behaves differently. It is demonstrated that the low Ra region corresponds to Darcy flow and the high to Forchheimer flow. Correlation equations for Nu for the Darcy regime are presented that account for viscous dissipation, and others for the Forchheimer regime that involve the first and second Forchheimer coefficients. The variation of properties with temperature and the wall effect on porosity (and consequently on heat transfer) are considered. The paper includes information concerning the resistance to flow in porous media that was obtained in conjunction with the heat transfer study.

INTRODUCTION

THE PRIMARY objective of the present investigation was to determine useful correlation equations for heat transfer by natural convection from horizontal cylinders embedded in porous media. This objective was accomplished by first obtaining a set of experimental heat transfer data and then analyzing this data in conjunction with an appropriate theory. In the course of this study it was found necessary to obtain certain information concerning the resistance to fluid flow exhibited by porous media. This fluid flow information is presented below following a review of literature that is relevant to the primary heat transfer problem.

REVIEW OF THE LITERATURE

Several analytical studies have been performed in recent years relating to the problem of steady two-dimensional natural convection about an infinitely long horizontal isothermal cylinder embedded in a porous medium of infinite extent. In most of these studies a curvilinear orthogonal coordinate system is used; furthermore, it is assumed that Darcy's law and the boundary-layer approximations are applicable, and that the gravitational force normal to the heated surface is negligible. With this formulation of the problem, Hardee [1] obtained the following expression for the Nusselt number based on the integral method:

$$Nu = 0.465\, Ra^{1/2} \tag{1}$$

where $Ra = Kg\beta\rho_\infty D\Delta T/\mu\alpha$ is called the Darcy-modified Rayleigh number.

More recently, Merkin [2] obtained similarity solutions for natural convection porous layers adjacent to axisymmetric and two-dimensional bodies of arbitrary shape. In an unpublished note, which will be reproduced in the next section, Cheng [3] has modified Merkin's analysis and applied it to the specific case of a horizontal isothermal cylinder. The result of this analysis is:

$$Nu = 0.565\, Ra^{1/2} \tag{2}$$

which differs from equation (1) only in the magnitude of the numerical coefficient.

Plumb and Huenefeld [4] have performed an analytical study of non-Darcy natural convection from vertical heated surfaces in porous media. More recently, Bejan and Poulikakos [5] analyzed the same problem in a manner that is relevant to the present study. Bejan and Poulikakos defined a new dimensionless group, $G = C_1\nu(C_2 g\beta\Delta T)^{-1/2}$, that they say "describes the extent to which the flow departs from Darcy flow". C_1 and C_2 are dimensional coefficients discussed in detail below. According to this criterion, the flow is governed by Darcy's law when G is large (100 or more) and gradually approaches non-Darcy flow as $G \to 0$. The authors also describe an intermediate regime when $G = O(1)$.

Bejan and Poulikakos deduce that for non-Darcy flow the Nusselt number for heat transfer by natural convection from an isothermal vertical wall in contact with a porous medium is given by the following equation:

$$Nu = 0.494(Ra_\infty)_y^{1/4} \tag{3}$$

where $(Ra_\infty)_y$ is a new Rayleigh number defined by

$$(Ra_\infty)_y = \frac{g\beta y^2\Delta T}{C_2\alpha^2}. \tag{4}$$

Here y denotes the vertical Cartesian coordinate. This new Rayleigh number should not be confused with the Darcy-modified Rayleigh number $(Ra)_y = Kg\beta y\Delta T/\nu\alpha$ used consistently in natural convection studies

NOMENCLATURE

A, B	Ergun constants
a, b, c	numerical constants
C	Darcy coefficient [K^{-1}]
C_1, C_2	Forchheimer coefficients
c_p	specific heat of fluid
d	diameter of glass spheres
D	diameter of test cylinder
Ge	Gebhart number, $g\beta D/c_p$
Gr	Grashof number, $Kg\beta D(T_s-T_\infty)/\nu^2$
g	gravitational constant
h	heat transfer coefficient
j	numerical constant
k	effective thermal conductivity
K	permeability
m, n	numerical constants
N	number of data points
Nu	Nusselt number, hD/k
p	pressure
P'	negative of pressure gradient
Pr	Prandtl number, $\mu c_p/k$
Q, q	heat transfer rate, heat flux
Ra	Darcy-modified Rayleigh number, $Kg\beta D(T_s-T_\infty)/\alpha\nu$
$(Ra)_{C_1}$	Forchheimer-modified Rayleigh number, $g\beta D(T_s-T_\infty)/C_1\alpha\nu$
Re	Reynolds number, Dv/ν
sech	hyperbolic secant
T	temperature
u, v	Darcian velocity components.

Greek symbols

α	effective thermal diffusivity
α_ε	function of porosity, $(1-\varepsilon)^2/\varepsilon^3$
β	coefficient of volumetric expansion of fluid
β_ε	function of porosity, $(1-\varepsilon)/\varepsilon^3$
Δ	temperature difference, T_s-T_∞
ε	porosity
κ	Kozeny–Carman constant
μ	dynamic viscosity of fluid
ν	kinematic viscosity, μ/ρ
ρ	fluid density
ψ	streamfunction.

Subscripts

calc	quantity determined by calculation
exp	quantity determined by experiment
s	refers to conditions on a heated surface
w	refers to wall effect
∞	refers to conditions far from a heated surface.

Error notation

E	percent error, $100(Nu_{exp}-Nu_{calc})/Nu_{exp}$
E(md)	percent mean deviation of error, $\sum_{i=1}^{N}\lvert E_i\rvert/N$
E(rms)	percent root mean square of error, $(\sum_{i=1}^{N}E_i^2/N)^{1/2}$.

involving Darcy flow. The subscript '∞' chosen for $(Ra_\infty)_y$ is intended to suggest that this new number becomes representative when the traditional $(Ra)_y$ becomes sufficiently large. Bejan and Poulikakos also present a solution for the case of uniform wall heat flux.

SIMILARITY SOLUTION FOR NATURAL CONVECTION WITH DARCY FLOW ABOUT AN ISOTHERMAL HORIZONTAL CYLINDER EMBEDDED IN A POROUS MEDIUM

This section reproduces an unpublished note by Cheng [3].

The problem of natural convection with Darcy flow about an isothermal horizontal cylinder embedded in a porous medium is, in general, not amenable to an analytical solution. A similarity solution for the problem is possible, however, if a curvilinear coordinate is used and the boundary-layer approximation is employed. To this end, the governing equations in cylindrical coordinates (r, θ) will first be transformed into a curvilinear orthogonal coordinate system (s, n) where s is the distance along the surface of the cylinder measured from the lower stagnation point and n is the distance perpendicular to the surface. These two coordinate systems are related by $r = R+n$ and $\theta = s/R$, where R is the radius of the cylinder. With these transformations, the governing equations in curvilinear orthogonal coordinates are

$$\frac{\partial u}{\partial s}+\frac{\partial}{\partial n}\left[\left(1+\frac{n}{R}\right)v\right]=0 \tag{5}$$

$$u=-\frac{K}{\mu}\left[\frac{R}{R+n}\frac{\partial p}{\partial s}+\rho g\sin\left(\frac{s}{R}\right)\right] \tag{6}$$

$$v=-\frac{K}{\mu}\left[\frac{\partial p}{\partial n}-\rho g\cos\left(\frac{s}{R}\right)\right] \tag{7}$$

$$\frac{R}{R+n}u\frac{\partial T}{\partial s}+v\frac{\partial T}{\partial n}=\alpha\left[\frac{R^2}{(R+n)^2}\frac{\partial^2 T}{\partial s^2}+\frac{\partial^2 T}{\partial n^2}+\frac{1}{(R+n)}\frac{\partial T}{\partial n}\right] \tag{8}$$

$$\rho=\rho_\infty[1-\beta(T-T_\infty)]. \tag{9}$$

Here u and v are the Darcian velocities in the s and n-directions, p is the pressure, T is the temperature, ρ is the density of the fluid, g is the gravitational acceleration, μ and β are the viscosity and thermal expansion

coefficient of the fluid, and α is the equivalent thermal diffusivity of the saturated porous medium. In this analysis viscous dissipation is neglected and hence does not appear in the energy equation, equation (8).

If it is assumed that the thermal boundary layer adjacent to the cylinder is thin such that $R \gg n$ within the thermal boundary layer, then equations (5), (6) and (8) can be approximated as follows:

$$\frac{\partial u}{\partial s} + \frac{\partial v}{\partial n} = 0 \tag{10}$$

$$u = -\frac{K}{\mu}\left[\frac{\partial p}{\partial s} + \rho g \sin\left(\frac{s}{R}\right)\right] \tag{11}$$

$$u\frac{\partial T}{\partial s} + v\frac{\partial T}{\partial n} = \alpha\left[\frac{\partial^2 T}{\partial n^2} + \frac{\partial T}{\partial n} + \frac{\partial^2 T}{\partial s^2}\right]. \tag{12}$$

Eliminating p from equations (7) and (11) by cross differentiation and neglecting the gravitational force normal to the surface leads to the following equation in terms of the streamfunction:

$$\frac{\partial^2 \psi}{\partial n^2} + \frac{\partial^2 \psi}{\partial s^2} = \frac{K\rho_\infty g\beta}{\mu} \sin\left(\frac{s}{R}\right)\frac{\partial T}{\partial n} \tag{13}$$

where the streamfunction is defined by

$$u = \frac{\partial \psi}{\partial n} \quad \text{and} \quad v = -\frac{\partial \psi}{\partial s}. \tag{14a,b}$$

Equation (9) in terms of the streamfunction is

$$\frac{\partial \psi}{\partial n}\frac{\partial T}{\partial s} - \frac{\partial \psi}{\partial s}\frac{\partial T}{\partial n} = \alpha\left[\frac{\partial^2 T}{\partial n^2} + \frac{\partial T}{\partial n} + \frac{\partial^2 T}{\partial s^2}\right]. \tag{15}$$

Equations (13) and (15) are the governing equations in a curvilinear coordinate system where the curvature effect has been neglected. Using the boundary-layer approximation, $\partial^2/\partial s^2 \ll \partial^2/\partial n^2$ and $\partial/\partial n \ll \partial^2/\partial n^2$, equations (13) and (15) become

$$\frac{\partial^2 \psi}{\partial n^2} = \frac{K\rho_\infty g\beta}{\mu} \sin\left(\frac{s}{R}\right)\frac{\partial T}{\partial n} \tag{16}$$

$$\frac{\partial^2 T}{\partial n^2} = \frac{1}{\alpha}\left(\frac{\partial \psi}{\partial n}\frac{\partial T}{\partial s} - \frac{\partial \psi}{\partial s}\frac{\partial T}{\partial n}\right). \tag{17}$$

For an isothermal cylinder, the boundary conditions are

$$n = 0: \quad \frac{\partial \psi}{\partial s} = 0, \quad T = T_s \tag{18a,b}$$

$$n \to \infty: \quad \frac{\partial \psi}{\partial n} = 0, \quad T = T_\infty. \tag{19a,b}$$

Equations (16) and (17) subject to the boundary conditions (18) and (19) admit a similarity solution of the form

$$\psi = \sqrt{\frac{K\rho_\infty \beta g(T_s - T_\infty)\alpha R}{\mu}}\left[1 - \cos\left(\frac{s}{R}\right)\right]^{1/2} f(\eta) \tag{20}$$

$$\theta(\eta) = \frac{T - T_\infty}{T_s - T_\infty} \tag{21}$$

$$\eta = \sqrt{\frac{K\rho_\infty \beta g(T_s - T_\infty)}{\mu\alpha R}}\,\frac{n \sin(s/R)}{\sqrt{1 - \cos(s/R)}} \tag{22}$$

where f and θ satisfy

$$f'' = \theta' \tag{23}$$

$$\theta'' + \frac{f\theta'}{2} = 0 \tag{24}$$

with boundary conditions given by

$$\theta(0) = 1, \quad f(0) = 0 \tag{25a,b}$$

$$\theta(\infty) = 0, \quad f'(\infty) = 0. \tag{26a,b}$$

It follows from equations (14a), (20) and (22) that the streamwise velocity is given by

$$u = \frac{K\rho_\infty \beta g \Delta T}{\mu} \sin\left(\frac{s}{R}\right) f'(\eta) \tag{27}$$

where $\Delta T = T_s - T_\infty$.

The preceding equation shows that the velocity at the surface of the cylinder u_s (corresponding to $\eta = 0$) is given by

$$u_s = \frac{K\rho_\infty \beta g \Delta T}{\mu} \sin\left(\frac{s}{R}\right) \tag{28}$$

where the condition $f'(0) = 1$ obtained from equations (23) and (25) has been employed.

Equations (23)–(26) are identical to the problem of natural convection about an isothermal flat plate in a porous medium which has been numerically integrated by Cheng and Minkowycz [6] who obtained $\theta(0) = -0.444$. With this value, the local surface heat flux is given by

$$q(x) = -k\left(\frac{\partial T}{\partial y}\right)_{y=0}$$

$$= 0.444k\Delta T\sqrt{\frac{K\rho_\infty g\beta\Delta T}{\mu\alpha R}}\,\frac{\sin(s/R)}{\sqrt{1 - \cos(s/R)}}. \tag{29}$$

The average heat flux can be obtained by integrating equation (29) to give

$$q = 0.565\,k(\Delta T)^{3/2}\sqrt{\frac{K\rho_\infty g\beta}{\mu\alpha D}} \tag{30}$$

which can be rewritten as

$$Nu = 0.565\,Ra^{1/2}. \tag{31}$$

It is relevant to note that (31) is derived based on Darcy's law with slip flow. Had the Brinkman model been used as the momentum equation with no-slip boundary conditions imposed, the value of Nu would be progressively lower than that given by (31) with increasing Rayleigh number. This lowering of Nu will be discussed in detail in a forthcoming paper.

RESISTANCE TO FLOW IN POROUS MEDIA

Introductory comments

In order to address the heat transfer problem with which this paper is primarily concerned it was

necessary to have prior knowledge of the resistance to the flow of fluids through porous media. The discussion of such flow resistance presented here is based upon previously published information and also upon recently obtained experimental evidence.

Most investigations of the resistance to flow in porous media are predicated upon the assumption that there exist two domains of the Reynolds number, Re: the 'lower' domain within which viscous forces predominate and Darcy's law holds, and the 'higher' domain within which inertial forces become significant and Darcy's law does not hold. However, as Bear [7] points out, there also exists a value of *Re below* which Darcy's law does not hold. The flow in this lowest range of Re will be referred to hereinafter as 'pre-Darcy flow', and the value of Re below which Darcy's law does not hold will be designated by Re_{DL}.* The existence of pre-Darcy flow is attributed to non-Newtonian behavior of fluids and the fact that the streaming potential generated by the flow, particularly in fine-grained media, can produce small countercurrents along the pore walls in a direction opposite to that of the main flow [7].

When a problem involves more than one of the domains discussed above, it becomes necessary to carefully delineate these domains, *and also the transition from one domain to the next.* Since, as will be shown, natural convection heat transfer in porous media constitutes just such a problem, the domains and transitions are discussed below, first in general terms and then quantitatively.

General discussion

Darcy's law for one-dimensional flow through porous media may be stated as follows:

$$P' = \left(\frac{\mu}{K}\right) v \tag{32}$$

where P' is the negative of the pressure gradient in the direction of flow, v is the volume rate of flow per unit cross-sectional area or 'Darcian speed' (or simply 'speed'),† μ is the viscosity of the fluid and K is a constant called the permeability of the porous medium. It will prove advantageous to multiply equation (32) by $d/\mu v$, where d is a characteristic dimension of the porous medium; thus

$$\frac{P'd}{\mu v} = \frac{d}{K} \tag{33a}$$

or

$$\frac{P'd}{\mu v} = Cd \tag{33b}$$

where $C = K^{-1}$ will be called the Darcy coefficient.

A great deal of analytical and experimental effort has been expended upon the determination of K for various porous media. The following semi-empirical equation has been found to accurately represent many experimental data:

$$K = (\kappa S_0^2 \alpha_\varepsilon)^{-1}; \quad \alpha_\varepsilon = \frac{(1-\varepsilon)^2}{\varepsilon^3} \tag{34}$$

where ε is the porosity, S_0 is the specific surface of the particles (surface area per unit volume) and κ is an experimentally determined dimensionless constant called the Kozeny–Carman constant. For a porous medium composed of spheres of uniform diameter $S_0 = 6/d$ and hence

$$K = \frac{d^2}{36\kappa\alpha_\varepsilon}. \tag{35}$$

For a given porous medium, there exists a value of $Re = Re_{DH}$, usually between 1 and 10, above which the flow deviates from Darcy's law; thus, Re_{DH} is the highest value of Re for which Darcy's law holds in a particular case. Darcy's law, when plotted using coordinates as shown in Fig. 1, is represented by the horizontal line labeled 'Eq. (33)'. In this figure the solid line represents (qualitatively) the actual behavior of the porous medium; thus, Darcy's law accurately represents the actual behavior of the porous medium from Re_{DL} to Re_{DH}. The pre-Darcy region is labeled 'I' in Fig. 1, and the Darcy region is labeled 'II'. An important and relevant aspect of pre-Darcy flow is that within this region a finite value of $P' = P'_0$ exists such that $v = 0$ when $P' < P'_0$. Thus, $P'D/\mu v$ exceeds all bounds when $P' < P'_0$. This behavior is indicated by the shape of the (truncated) solid line in Fig. 1 for $Re < Re_{DL}$.

If Re continually increases above Re_{DH} a range is

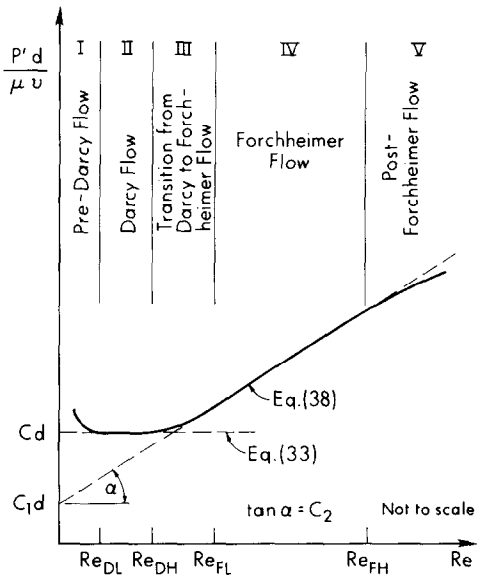

FIG. 1. Graph of $P'd/\mu v$ vs Re for porous media.

*The subscript DL is a mnemonic device which refers to the lowest value (L) of the Reynolds number for which Darcy flow (D) occurs. Similar subscripts will be used to refer to the highest value (H) of the Reynolds number for which a particular kind of flow occurs.

†The term 'velocity' will be used in this connection when the context makes the intended meaning clear.

eventually encountered, designated by IV in Fig. 1 and defined by $Re_{FL} \leqslant Re \leqslant Re_{FH}$, wherein Forchheimer's equation represents the flow:

$$P' = (C_1\mu)v + (C_2\rho)v^2. \tag{36}$$

Here C_1 and C_2 are dimensional constants that will be referred to hereinafter as the first and second Forchheimer coefficients. The quadratic term in (36) is attributed to inertial effects. Ergun has suggested that the Forchheimer coefficients can be expressed as follows:

$$C_1 = \frac{A\alpha_\varepsilon}{d^2}; \quad \alpha_\varepsilon = \frac{(1-\varepsilon)^2}{\varepsilon^3} \tag{37a}$$

and

$$C_2 = \frac{B\beta_\varepsilon}{d}; \quad \beta_\varepsilon = \frac{(1-\varepsilon)}{\varepsilon^3} \tag{37b}$$

where A and B are universal experimentally-determined dimensionless constants (referred to hereinafter as the first and second Ergun constants), d is a characteristic dimension, and ε is the porosity of the medium. As was done in the case of Darcy's law, equation (36) can be multiplied by $d/\mu v$ with the result:

$$\frac{P'd}{v} = C_1 d + C_2 Re \tag{38a}$$

or

$$\frac{P'd}{\mu v} = \frac{A\alpha_\varepsilon}{d} + \frac{B\beta_\varepsilon Re}{d}. \tag{38b}$$

A plot of equation (38) is the inclined straight line in Fig. 1. The flow for which (38) represents the actual behavior of a porous medium will hereinafter be called Forchheimer flow, corresponding to region IV in Fig. 1, with lower and upper bounds Re_{FL} and Re_{FH}. Between the regions of Darcy flow (II) and Forchheimer flow (IV) is a transition region, labeled 'III' in Fig. 1, with lower and upper bounds Re_{DH} and Re_{FL}.

The curve representing transition from Darcy to Forchheimer flow (region III of Fig. 1) represents a problem *vis-à-vis* the analysis of data because the equation of this curve is a complex function (compared to the functions in both the Darcy and Forchheimer domains). This problem can be avoided without incurring significant error by assuming that Darcy's law holds beyond Re_{DH} to a value designated by Re_{DF} at which point fully-developed Forchheimer flow is assumed to occur. Thus, Re_{DF} represents an (artificial) point of abrupt transition from Darcy to Forchheimer flow.

Experiments conducted in conjunction with the present investigation reveal the existence of a region labeled 'V' in Fig. 1, called post-Forchheimer flow, in which turbulence effects become significant and, at sufficiently high values of Re, dominate the flow. The symbol Re_{FT} represents an (artificial) point of abrupt transition from Forchheimer to turbulent flow. Since the velocities attained in the heat transfer experiments reported in this paper are well below those needed to achieve turbulent flow, this region will not be discussed here in detail.

Quantitative information

The porous media used in the present study consisted of matrices of small soda-lime glass spheres saturated with either water or 20 Cs silicone oil. Formulas for the relevant thermophysical properties of this oil are provided in [8, Appendix]. The nominal diameters of the glass spheres were 2, 3 and 4 mm. Kim [9] packed quantities of each of these three sizes of glass spheres into the test section (8.66 cm I.D. by 45.72 cm long) of a water tunnel and determined the resistance to flow in these porous media by accurately measuring the pressure drop across the test section corresponding to different imposed velocities of flow of water. The temperature of the flowing water was measured in order to ascertain its viscosity and density. The relevant results determined from these measurements are displayed in Table 1. The entries in Table 1 incorporate corrections designed to compensate for the 'wall effect' caused by the unavoidable non-random distribution of glass spheres near a boundary. Table 1 does not contain a value for Re_{DL} because the apparatus used by Kim could not accurately measure the extremely low pressure gradients and velocities that pertain to pre-Darcy flow. The values of the parameters listed in Table 1 were used in the subsequent analysis of the heat transfer data obtained in this study.

HEAT TRANSFER APPARATUS AND EXPERIMENTAL PROCEDURE

The heat transfer measurements made in the present study were performed using the electrically-heated test specimen and thermally-insulated cylindrical stainless-steel tank (0.1945 m I.D. by 1.27 m high) described in [8]. The test specimen was inserted diametrically in the tank between two vertical baffle plates as shown in Figs. 2 and 3. The test specimen (1.45 cm O.D.) has an independently-heated central test section that is 2.540 cm long flanked by a pair of contiguous independently heated 'guard' sections, each of which is 3.050 cm long. Thus, the overall heated length of the test specimen is 8.650 cm, which equals the distance between the vertical baffles in the tank. Heat transfer data were recorded only for the centrally-located test section. The purpose

Table 1. Information on the resistance to flow in porous media

d(m)	0.002098	0.003072	0.004029
ε	0.3570	0.3600	0.3580
$Cd(m^{-1} \times 10^{-5})$	8.321	5.497	4.289
$K(m^2 \times 10^9)$	2.521	5.589	9.395
$C_1 d(m^{-1} \times 10^{-5})$	7.879	5.204	4.060
$C_2(m^{-1} \times 10^{-3})$	12.93	8.578	6.671

$\kappa = 5.34$, $Re_{DH} = 2.1 \pm 0.1$, $Re_{DF} = 3$, $A = 182$, $B = 1.92$, $Re_{FL} = 5.0 \pm 0.5$, $Re_{FT} = 100$, $Re_{FH} = 80 \pm 5$.

of the guarded test section design and baffle arrangement was to create experimental conditions that closely approximate the two dimensional temperature and velocity fields corresponding to an 'ideal' infinitely long heated cylinder in an infinite medium. That this experimental system does, indeed, closely approximate the ideal case for *natural convection in liquids*, was verified as reported in [8]; whether the approximation is also close in the present case involving *porous media* was investigated by performing certain experiments described below.

The steady-state bulk temperature of the porous medium, T_∞, was measured by means of a single thermocouple located directly below the test specimen as shown in Fig. 2. The steady-state surface temperature, T_s, of the test section, corresponding to arbitrarily imposed overall rates of heat dissipation Q, was measured by averaging the readings of two thermocouples located below the surface of the test section and correcting this average by subtracting the temperature drop due to the radial conduction of heat to the surface. Since the test specimen has a copper core, it is nearly isothermal. In order to reduce the errors introduced by the small variation of the temperature difference $\Delta T = (T_s - T_\infty)$ around the periphery of the test section upon the reported results, the specimen was rotated around its axis and left in that angular position which corresponds to a value of ΔT equal to the integrated mean value of ΔT for a complete revolution, as was done in [8]. During this procedure the tank contained only liquid (water) because the presence of a porous medium would have prevented the rotation of the test specimen.

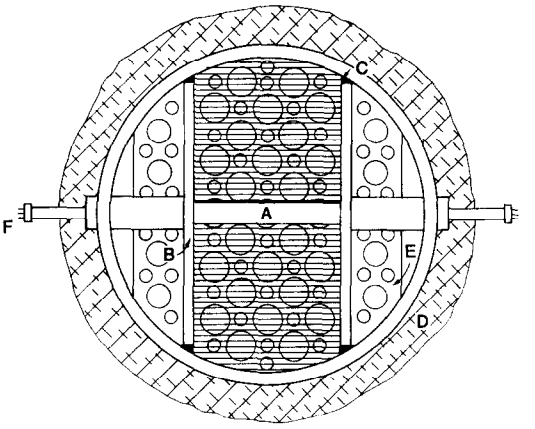

A. Test Cylinder
B. Stainless Steel Baffles
C. Silicone Rubber Seal
D. Insulated Tank Wall
E. Perforated Bottom Plate
F. Electrical Leads

FIG. 3. Schematic top view of experimental apparatus.

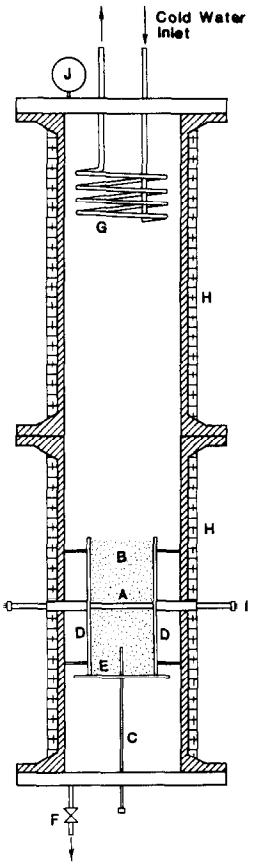

A. Test Cylinder
B. Porous Medium Reservoir
C. Thermocouple Probe
D. Stainless Steel Baffles
E. Perforated Bottom Plate
F. Drain
G. Heat Exchanger Coil
H. Thermally Insulated Tank
I. Electrical Leads
J. Pressure Gauge

FIG. 2. Schematic vertical cross-sectional view of experimental apparatus.

The volume of the tank contained between the vertical baffle plates was filled with glass spheres to various depths, and this space became the porous medium (called 'porous reservoir') when the tank was filled with water or oil. The porous reservoir was bounded below by a perforated stainless-steel plate covered by screening material which supported the glass spheres yet allowed the flow of fluid upward into the porous reservoir. The space in the tank outside the porous reservoir allowed recirculation of fluid. A coiled heat exchanger installed near the top of the tank as shown in Fig. 2 removed the heat dissipated by the test specimen. The tank was pressurized to about 5 atm when tests using water were performed, in order to prevent the formation of bubbles of vapor or air. Tests employing oil were performed at atmospheric pressure.

The physical characteristics of the three sizes of glass spheres (nominal diameters: 2, 3 and 4 mm) used to create the porous media employed in this study were analyzed by Phan [10]. By carefully measuring the density of the spheres and weighing individually a statistically large number (100 or more) of each size on a high precision balance, Phan determined that the average equivalent mean diameters of the three sizes were 2.098, 3.072 and 4.029 mm, respectively. He also determined the following formula for the thermal conductivity of the spheres, based upon published information for soda-lime glass:

$$k_s = 1.00416 + 1.6736 \times 10^{-3} T - 4.184 \times 10^{-6} T^2 \quad (39)$$

where T is the temperature in °C and k_s is expressed in W m^{-1} °C^{-1}.

The effective conductivity of a porous medium was *defined* by the following formula:

$$k = \varepsilon k_f + (1-\varepsilon)k_s \quad (40)$$

where ε is the porosity and k_s and k_f represent the thermal conductivities of the glass spheres and saturating fluid, respectively.

Two kinds of heat transfer experiments were performed. The objective of the first kind, called 'preliminary tests', was to determine whether the porous reservoir was sufficiently large to adequately represent an infinite medium; the second kind, called 'primary tests', consisted of steady-state measurements of T_s and T_∞ corresponding to various imposed overall rates of heat transfer Q. The temperature measurements made are estimated to be correct to within 0.03°C, and the measurements of Q are correct to within 0.1%.

A sketch which shows graphically the definitions of certain spatial parameters used for the preliminary tests is shown in Fig. 4. As indicated, the distance W denotes half the width of the porous reservoir, H_1 denotes the height of the reservoir above the centerline of the test specimen, and H_2 denotes the depth of the reservoir below the centerline of the test cylinder whose diameter is denoted by D. The total height H of the porous reservoir is equal to $(H_1 + H_2)$ and the maximum value of H equals the height B of the baffle plates. Two sets of baffles were used having lengths $B = 25$ and 50 cm, respectively. Since $H_2 = B/2$ in all cases, the use of these two sets of baffles provided two experimental values of H_2 and, consequently, two values of H_2/D, specifically, 11.1 and 22.2. Both sets of baffles had the same width, which was selected so as to insure that the distance between the baffles was equal to the total heated length (8.640 cm) of the test cylinder; thus, the distance between baffles was not varied in these tests. The values of H_1 and W and, consequently, of H_1/D and W/D, were varied between fairly wide limits as described in the following.

It was easy to vary H_1/D experimentally—the space between the baffles was simply filled with glass spheres until the desired value of H_1 was attained. The experimental range of H_1/D was from 1.1 to 11.1. In order to vary W experimentally, a number of solid plastic bars were placed between the baffles symmetrically with respect to the test specimen as shown in Fig. 4. The bars had lengths equal to B (25 cm), widths equal to the distance between baffles (8.64 cm) and thickness equal to 1.27 cm (0.5 in.). The value of W was changed (increased) by withdrawing the plastic bars symmetrically in pairs and filling the space previously occupied by the bars with glass spheres. The experimental range of W/D was from 1.2 to 8.5.

The purpose of varying the spatial parameters defined above was to determine experimentally the minimum values of the parameters above which the heat transfer data would become independent of these parameters. It was reasoned that, if all minimum values of the spatial parameters were exceeded in an experiment—the satisfaction of these conditions constitutes what will be called a 'criterion for an infinite porous medium'—then, for this experiment, the porous

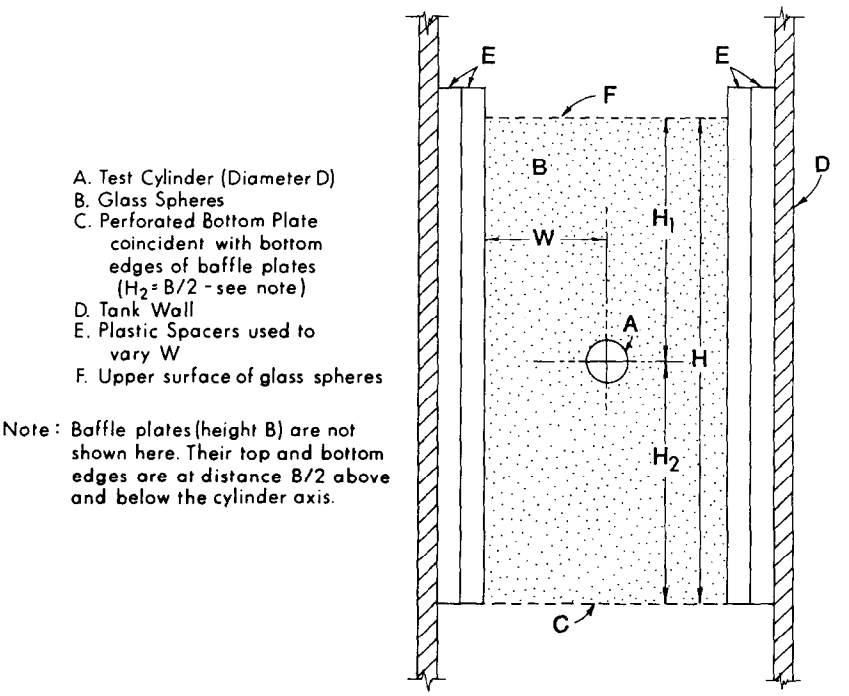

FIG. 4. Sketch of porous medium reservoir showing definitions of certain special parameters.

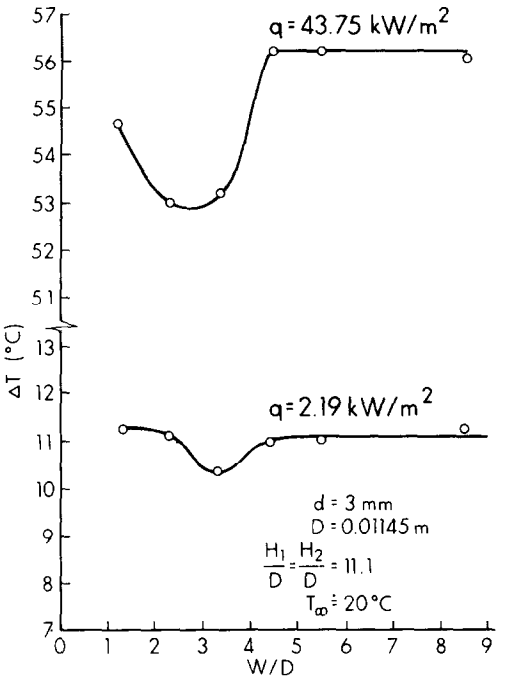

FIG. 5. Plot of ΔT vs W/D for two values of q.

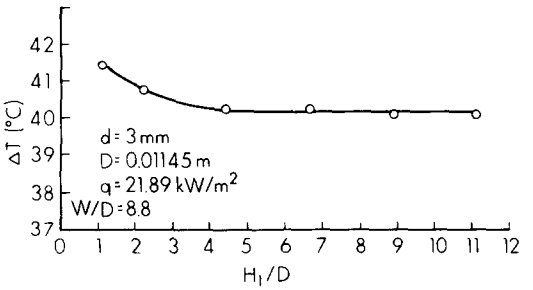

FIG. 6. Plot of ΔT vs H_1/D.

reservoir closely approximated the ideal case of an infinite medium.

EXPERIMENTAL RESULTS AND DISCUSSION

Preliminary data

Figure 5 shows graphically the results of the preliminary tests made with water as the saturation fluid and with varying W/D for two different values of heat flux q and with $H_1/D = H_2/D = 11.1$. The behavior of ΔT in both cases is qualitatively similar: the curves for ΔT have local minima, which implies an enhanced heat transfer coefficient,* and ΔT is very nearly constant for $W/D \geqslant 4.4$. Figure 6 is a plot of ΔT vs H_1/D for $W/D = 8.8$ and $q = 21.99$ k W m^{-2}. Here, too, ΔT is very nearly constant when the spatial parameter, in this case H_1/D, is equal to or greater than 4.4. A pair of tests with the same q and $H_2/D = 11.1$ and 22.2 (and with $H_1/D = H_2/D$) yielded identical measurements of ΔT. No preliminary tests were performed with oil.

Primary data

The primary heat transfer tests were conducted in porous reservoirs with $W/D = 8.8$ and $H_1/D = H_2/D = 11.1$ or 22.2; therefore, based upon the results of the preliminary tests reported above, the 'criterion for an infinite porous medium' was satisfied for experiments with water insofar as the values of W, H_1, and H_2 are concerned. However, the distance between the baffles (8.640 cm) could not be varied in the present study due to the physical limitations of the apparatus. Therefore, the criterion for an infinite porous medium could not be conclusively established relative to distance along the axis of the test specimen. However, judging from the results of the preliminary tests with varying W, it is concluded that the porous reservoirs used to obtain the primary water data of this study approximate infinite media sufficiently well as to render these data representative of the corresponding ideal case.

The primary heat transfer data and relevant dimensionless parameters are listed in Tables 2 and 3. All thermophysical properties that appear in dimensionless parameters were evaluated in this study at reference temperatures defined as follows:

$$T_j = T_\infty + j(T_s - T_\infty); \quad 0 \leqslant j \leqslant 1. \tag{41}$$

Obviously, when $j = 0.5$, T_j is the mean film temperature. The reference temperatures employed herein are identified by specifying the value of j. In Tables 2 and 3 the test identifier (ID) consists of a number followed by a letter (S or W) plus another digit (2, 3 or 4). The letter S refers to tests conducted with 20 Cs silicone oil as the fluid medium and W refers to tests conducted with water. The final digit refers to the nominal glass sphere diameter (in millimeters) used to form the porous matrix for the indicated test; thus, for example, the sequence 9W3 identifies the ninth test performed using water as the fluid medium and 3-mm glass spheres as the matrix of the porous medium.

First correlation: j = 0.5. Based upon the theoretical result embodied in equation (31) and also upon previously published correlation equations for natural convection from horizontal cylinders (for example, as reported in [8]), it was conjectured that at least some of the data listed in Table 2, could be correlated by an equation of the form:

$$Nu = c\, Ra^a\, Pr^b; \quad j = 0.5 \tag{42}$$

where c, a and b are constants, Ra is the Darcy-modified Rayleigh number and Pr is the Prandtl number.

In order to determine for which tests (42) would represent the data, and, having done so, to then determine the numerical values of the constants, the following procedure was followed. First, a log–log graph of all the experimental values of Nu vs Ra was

*This enhancement has been dubbed the 'chimney effect'. Sparrow and Pfeil [11] have reported a similar effect.

Table 2. Experimental data and heat transfer parameters for $j = 0.5$

Test ID*	T_s (°C)	T_∞ (°C)	h (W m^{-2} °C^{-1})	Nu	Ra	Pr	$(Re)_{max}$	$Ge \times 10^9$
1W2	28.45	22.20	69.52	0.8968	2.424	4.163	0.1068	6.949
2W2	31.80	21.81	109.0	1.403	4.212	4.016	0.1924	7.331
3W2	36.03	22.05	155.7	1.996	6.627	3.808	0.3194	7.890
4W2	44.33	21.81	241.8	3.080	12.91	3.473	0.6832	8.847
5W2	53.51	21.93	344.8	4.359	21.95	3.140	1.287	9.876
6W2	66.71	22.05	487.5	6.104	39.44	2.744	2.653	11.23
7W2	85.34	22.05	688.1	8.507	74.14	2.310	5.949	12.95
1W3	21.11	20.13	33.50	0.4364	0.623	4.696	0.03561	5.662
2W3	22.35	20.92	38.27	0.4975	0.977	4.574	0.05729	5.949
3W3	26.05	21.36	92.64	1.200	3.665	4.340	0.2267	6.518
4W3	29.25	21.68	143.9	1.858	6.572	4.155	0.4248	6.985
5W3	32.81	21.47	192.0	2.472	10.81	3.989	0.7279	7.416
6W3	39.28	21.24	301.9	3.868	20.16	3.707	1.463	8.187
7W3	47.47	21.72	422.8	5.380	35.01	3.363	2.803	9.193
8W3	58.35	20.68	578.0	7.299	62.24	3.029	5.544	10.26
9W3	76.52	21.31	788.8	9.828	125.0	2.521	13.43	12.09
10W3	91.77	21.19	925.7	11.42	197.9	2.205	24.40	13.42
1W4	22.42	21.66	43.20	0.5607	0.896	4.523	0.06972	6.062
2W4	21.98	20.87	49.30	0.6405	1.255	4.595	0.09612	5.890
3W4	24.82	21.36	125.6	1.627	4.368	4.403	0.3493	6.351
4W4	27.73	21.93	187.8	2.425	8.148	4.216	0.6806	6.818
5W4	28.63	19.95	250.9	3.244	11.81	4.273	0.9734	6.675
6W4	35.35	20.97	378.7	4.864	24.30	3.890	2.202	7.673
7W4	42.46	21.72	525.0	6.699	42.42	3.552	4.215	8.620
8W4	54.28	21.24	659.0	8.336	85.77	3.139	9.663	9.885
9W4	79.17	21.49	944.0	11.73	228.8	2.454	33.14	12.35
1S3	24.92	21.91	36.11	0.5757	0.169	38.76	0.001173	73.36
2S3	29.97	22.15	41.73	0.6632	0.459	36.75	0.003366	73.40
3S3	34.57	22.70	45.84	0.7262	0.727	34.92	0.005621	73.44
4S3	44.61	22.68	49.64	0.7815	1.456	31.68	0.01246	73.52
5S3	60.05	22.78	58.43	0.9118	2.791	27.40	0.02783	73.65
6S3	69.81	23.09	69.86	1.084	3.772	25.02	0.04136	73.73
7S3	83.30	22.42	89.46	1.379	5.391	22.37	0.06657	73.83
8S3	95.86	20.40	108.3	1.660	7.192	20.47	0.09776	73.92
9S3	110.8	23.04	124.1	1.877	9.409	17.74	0.1484	74.07

*The first digit indicates the test number; W = water, S = 20 Cs silicone oil; the final digit indicates the nominal glass-sphere diameter (mm).

made. This graph revealed that, within a certain portion of the overall experimental range of Ra, the plotted points defined a pair of straight lines, one for water and one for oil. These particular points (23 in number: one through 6W2; one through 7W3; one through 6W4; six through 9S3) were then used to find the optimum values of the numerical constants in equation (42) using a computer regression program. The optimum values of the constants were found to be $c = 0.679$, $a = 0.646$ and $b = -0.126$ with which (42) becomes

$$Nu = 0.679\ Ra^{0.646}\ Pr^{-0.126};\quad j = 0.5. \qquad (43)$$

Figure 7 shows a log–log plot of $Nu\ Pr^{0.126}$ vs Ra for all the data in Table 2. This figure reveals that the overall range of Ra can be subdivided into two subranges, designated 'low' (Ra less than approx. 40) and 'high', within each of which the heat transfer parameter $Nu \cdot Pr^{0.126}$ behaves differently. The 23 data points for which equation (43) is an accurate representation fall in the low range. It was hypothesized that Darcy flow occurs in the low range of Ra and that Forchheimer flow occurs in the high range, wherein the seven 'high' data points 7W2; 8, 9,10W3; 7, 8, 9W4 lie. The validity of this hypothesis was tested by determining for each heat transfer test a representative Reynolds number, designated by $(Re)_{max}$, based upon the characteristic diameter of the glass spheres d and the maximum velocity along the surface of the test specimen, designated by u_{max} and calculated from equation (28) to be as follows:

$$u_{max} = \frac{K\beta g \Delta T}{\nu};\quad j = 0.5. \qquad (44)$$

Thus,

$$(Re)_{max} = \frac{Kd\beta g \Delta T}{\nu^2};\quad j = 0.5. \qquad (45)$$

If $(Re)_{max}$ is chosen successively equal to $Re_{DF} = 3.0$ and $Re_{FT} = 100$, then equation (45) provides the following criteria for determining whether Darcy or Forchheimer

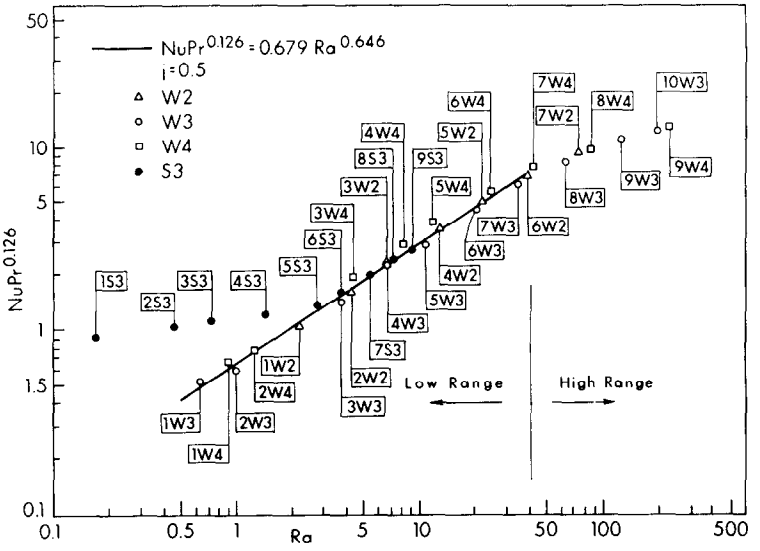

FIG. 7. Log–log plot of $Nu\ Pr^{0.126}$ vs Ra; $j = 0.5$.

theory is applicable:

$$\text{for Darcy theory: } Re_{DL} < (Re)_{max} \leqslant 3^* \quad (46)$$

$$\text{for Forchheimer theory: } 3 < (Re)_{max} \leqslant 100. \quad (47)$$

The values of $(Re)_{max}$ listed in Table 2 confirm the hypothesis that Forchheimer theory is applicable to the seven 'high' data points and Darcy theory is applicable to the rest of the data. The deviation of the seven 'high' data points from the straight line in Fig. 7 can be attributed to the combined inertia effect and the no-slip boundary condition mentioned below equation (31). It is easily shown that $(Ra)_{max} = DPr(Re)_{max}/d$.

It may be worthwhile to mention that equations (46) and (47) can be converted into equivalent statements involving a suitably defined Rayleigh number, $(Ra)_{max}$; however, this is not only superfluous but possibly misleading, inasmuch as it is the *Reynolds number*—not the Rayleigh number—that is the primary determinant of the kind of flow that exists in a particular situation.

Having established the applicability of Forchheimer theory to the seven 'high' data points, these data were then correlated by adopting the following hypothesis:

$$Nu\ Pr^{0.126} = c(Ra)_{C_1}^{a}\left(\frac{C_1 D}{C_2}\right)^{b} \quad (48)$$

where c, a and b are constants and

$$(Ra)_{C_1} = \frac{g\beta D\Delta T}{C_1 \alpha v}$$

is obtained from the Darcy-modified Rayleigh number

*The precise value of Re_{DL} is not available but published information on Darcy flow indicates that $Re_{DL} < 1 \times 10^{-5}$, which is far below $(Re)_{max}$ for any of the data obtained in the present study.

Table 3. Heat transfer parameters for $j = 0.32$

Test ID*	Nu	Ra	Pr	$(Re)_{max}$	$Ge \times 10^9$
1W2	0.8985	2.268	4.281	0.09712	6.651
2W2	1.407	3.804	4.196	0.1662	6.865
3W2	2.005	5.803	4.043	0.2633	7.259
4W2	3.100	10.66	3.810	0.5137	7.885
5W2	4.398	17.28	3.555	0.8933	8.607
6W2	6.178	29.40	3.234	1.673	9.579
7W2	8.642	52.08	2.859	3.359	10.82
1W3	0.4365	0.615	4.718	0.0350	5.612
2W3	0.4977	0.959	4.605	0.05591	5.877
3W3	1.202	3.474	4.433	0.2103	6.289
4W3	1.862	6.062	4.297	0.3787	6.625
5W3	2.481	9.637	4.192	0.6173	6.889
6W3	3.889	17.08	4.002	1.147	7.384
7W3	5.420	28.36	3.733	2.043	8.115
8W3	7.376	47.23	3.504	3.628	8.770
9W3	9.969	89.40	3.063	7.873	10.14
10W3	11.167	135.6	2.781	13.18	11.12
1W4	0.5608	0.888	4.538	0.06883	6.024
2W4	0.6408	1.237	4.618	0.09430	5.834
3W4	1.629	4.196	4.473	0.3302	6.180
4W4	2.429	7.650	4.327	0.6225	6.540
5W4	3.253	10.71	4.444	0.8484	6.252
6W4	4.885	21.09	4.140	1.795	7.013
7W4	6.740	35.40	3.872	3.223	7.722
8W4	8.413	66.73	3.574	6.589	8.555
9W4	11.90	162.6	3.000	19.19	10.34
1S3	0.5761	0.1680	39.19	0.001149	73.35
2S3	0.6644	0.4490	37.80	0.003193	73.38
3S3	0.7281	0.7020	36.43	0.005192	73.41
4S3	0.7853	1.367	34.20	0.01080	73.46
5S3	0.9188	2.517	31.05	0.02200	73.54
6S3	1.094	3.323	29.16	0.03102	73.59
7S3	1.395	4.593	27.16	0.04623	73.66
8S3	1.684	5.923	25.89	0.06282	73.70
9S3	1.916	7.579	23.05	0.09061	73.81

*Symbols as Table 2.

by replacing $K(=1/C)$ with $1/C_1$—this parameter, which will be called the Forchheimer-modified Rayleigh number, represents the influence of the linear velocity term in Forchheimer's equation upon the rate of heat transfer. The dimensionless quantity (C_1D/C_2) represents the influence of the quadratic velocity term in Forchheimer's equation—its contribution can be regarded as being a modification of the effect of the linear term. This reasoning is analogous to that proposed by Bejan and Poulikakos, who regard their parameter G as a factor that represents a degree of deviation from the Darcy solution. The factor $Pr^{0.126}$ in equation (48) was adopted from equation (43). The optimum values of c, a and b in (48) were found to be 2.05, 3.17 and 0.0226, respectively, with which the correlation becomes

$$Nu\,Pr^{0.126} = 2.05\,(Ra)_{C_1}^{0.317}\left(\frac{C_1D}{C_2}\right)^{0.0226}; \quad j = 0.5. \tag{49}$$

Equation (49) is valid for $3 < (Re)_{max} \leqslant 100$. A graph of equation (49) together with the relevant experimental data is shown in Fig. 8. The errors incurred by (49) with respect to the relevant experimental data are listed in Table 4. (See Nomenclature for error notation.)

Equations (43) and (49) adequately correlate all the experimental data plotted in Fig. 7 except for the first four or five oil points (1–5S3). These oil data exhibit a markedly different trend from the rest of the data that lie in the low range of Ra. They were successfully correlated by pursuing a suggestion made in the closing sentence of ref. [12] to the effect that viscous dissipation might be significant in the case of natural convection in porous media.

In order to identify a measure of viscous dissipation in the present context, the energy equation, appropriately modified for natural convection in porous media and including the viscous dissipation term expressed in terms of Darcy's law, was examined. For present purposes it was sufficient to consider the steady one-dimensional energy equation which is derived in the recent text by Bejan [13] and is

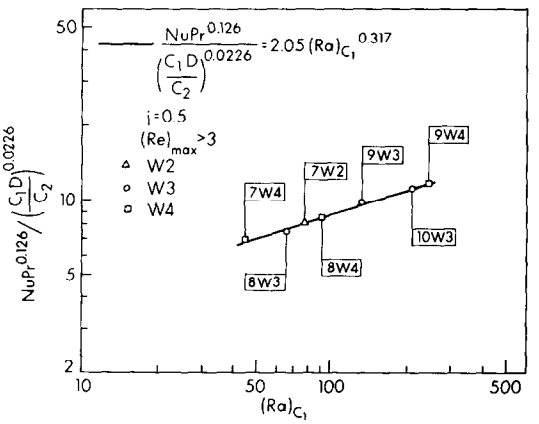

FIG. 8. Graph of equation (49) and relevant data.

Table 4. Errors incurred by correlation equations with respect to relevant experimental data

	E(md)	E(rms)
Darcy regime		
Equation (59); $j = 0.5$	5.01	6.75
Equation (60); $j = 0.32$	4.88	6.20
Equation (63); $j = 0.5$, ε_w	4.64	5.99
Equation (64); $j = 0.32$, ε_w	4.45	5.75
Forchheimer regime		
Equation (49); $j = 0.5$	1.27	1.90
Equation (61); $j = 0.32$	1.25	1.86
Equation (65); $j = 0.5$, ε_w	1.26	1.79
Equation (66); $j = 0.32$, ε_w	1.27	1.74

reproduced here as follows:

$$v\frac{\partial T}{\partial x} = \frac{k}{\rho c_p}\frac{\partial^2 T}{\partial x^2} + \frac{vv^2}{K\rho c_p} \tag{50}$$

where v is the velocity in the x-direction.

Equation (50) was rendered non-dimensional by means of the following transformations:

$$V = \frac{v}{V_c}, \quad X = \frac{x}{D_c} \quad \text{and} \quad \phi = \frac{T - T_\infty}{T_s - T_\infty},$$

where D_c is a characteristic length and

$$V_c = \frac{Kg\beta(T_s - T_\infty)}{\nu}$$

is taken as the characteristic velocity [see equation (28)]. When each term in equation (50) is transformed via the preceding dimensionless quantities, the result is

$$\frac{Kg\beta(T_s - T_\infty)^2}{\nu D_c} V\frac{\partial \phi}{\partial X} = \frac{k(T_s - T_\infty)}{\rho c_p D_c^2}\frac{\partial^2 \phi}{\partial X^2} + \frac{\nu}{Kc_p}\left(\frac{Kg\beta\Delta T}{\nu}\right)^2 V^2. \tag{51}$$

Multiplying equation (51) by $D_c^2/(\nu\Delta T)$ yields

$$Gr\,V\frac{\partial \phi}{\partial X} = \frac{1}{Pr}\frac{\partial^2 \phi}{\partial X^2} + Ge\,Gr(V^2) \tag{52}$$

where

$$Gr = \frac{Kg\beta D_c(T_s - T_\infty)}{\nu^2} \quad \text{is the Grashof number,}$$

$$Pr = \frac{\mu c_p}{k} \quad \text{is the Prandtl number,}$$

and

$$Ge = \frac{g\beta D_c}{c_p} \quad \text{is the Gebhart number.}$$

Equation (52) indicates that the temperature distribution depends only upon Gr, Pr and Ge. Consequently, the Nusselt number depends upon these same parameters; that is,

$$Nu = f(Gr, Pr, Ge). \tag{53}$$

According to the theory of dimensional analysis, an alternative equivalent statement to equation (51) is

$$Nu = g(Ra, Pr, Ge) \tag{54}$$

since $Ra = Gr\,Pr$. The Gebhart number, which was also employed in [12], is the sought-for measure of viscous dissipation. The value of Ge for the silicone oil used here is approx. 10 times its value for water. This disparity in the value of Ge reveals why viscous dissipation for the present water experiments is negligible compared with its magnitude for the oil experiments.

Having identified a parameter that characterizes the viscous dissipation, the following hypothesis was adopted in order to correlate the errant oil data:

$$Nu\,Pr^{0.126} = 0.679\,Ra^{0.646} + \Delta; \quad j = 0.5 \tag{55}$$

where $\Delta = f(Ge)g(Ra)$ and D_c is taken to be the cylinder diameter D. This hypothesis is predicated upon the assumption that the ordinates of the first five oil data points in Fig. 7 differ from the predictions of equation (43) by an amount Δ, and that Δ can be represented by a function of Ge multiplied by a function of Ra. Next, it was hypothesized that

$$f(Ge) = m\,Ge^n \tag{56}$$

where m and n are constants to be determined from experimental data. The present experimental data are insufficient to definitely determine the values of m and n, because Ge is nearly constant for the oil data under consideration and nearly negligible, by comparison, for the water data; therefore, all the oil data taken together represent a single datum for evaluating m and n—this point will be discussed further below. If n is arbitrarily chosen equal to 1, then

$$f(Ge) = m\,Ge\,g(Ra). \tag{57}$$

Now, Δ can be calculated for each oil datum under consideration using (43), and so a plot of Δ vs Ra can be constructed. This was done and it was recognized and verified that Δ is closely approximated by

$$\Delta = m\,Ge\,\text{sech}\,Ra. \tag{58}$$

where $m = 9.79 \times 10^6$. Hence, finally, equation (55) becomes

$$Nu\,Pr^{0.126} = 0.679\,Ra^{0.646} + m\,Gr\,\text{sech}\,Ra; \quad j = 0.5 \tag{59}$$

where $m = 9.79 \times 10^6$ *if* $n = 1$.

Equation (59) is valid for $0.001 < (Re)_{max} \leqslant 3$. The errors incurred by (59) with $n = 1$ are listed in Table 4; A graph of (59) together with the relevant data points is shown in Fig. 9.

In concluding this discussion of equation (59), it is emphasized that the values of the constants m and n contained therein have not been uniquely determined. Thus, if n were chosen equal to 2, an equally representative correlation could have been determined which would contain a different (compensating) value of m. The definitive determination of m and n can be accomplished only if additional heat transfer data with different values of Ge become available.

Second correlation: j = 0.32. It was shown in [8] that the influence of property variation on heat transfer by natural convection from horizontal cylinders can be taken into account more accurately by evaluating properties at $j = 0.32$ than by evaluating them at $j = 0.5$ (the mean film temperature). In the present study it was found that $j = 0.32$ also yields improved results. With $j = 0.32$ the correlation procedures described above yield:

$$Nu\,Pr^{0.0896} = 0.643\,Ra^{0.694} + 8.40 \times 10^6 Ge\,\text{sech}\,Ra; \quad 0.001 < (Re)_{max} \leqslant 3 \tag{60}$$

and

$$Nu\,Pr^{0.0896} = 0.986\,(Ra)_{C_1}^{0.372}\left(\frac{C_1 D}{C_2}\right)^{0.131}; \quad 3 < (Re)_{max} \leqslant 100. \tag{61}$$

The errors incurred by equations (60) and (61) are listed in Table 4.

Third correlation: the wall effect. It was observed that the errors incurred by the correlation equations presented above were greatest for the data obtained with the 4-mm glass spheres. This was attributed to the influence of the so-called 'wall effect', which is caused by the fact that the glass spheres of the porous medium are in point contact with (tangential to) the surface of the test specimen, and this results in a large increase in ε near the heat transfer surface. In order to take the wall effect into account, at least partially, the value of ε that appears in all correlation calculations was replaced by a 'wall corrected porosity' ε_w defined as follows:

$$\varepsilon_w = \varepsilon\left[1 + \frac{1}{2}\left(\frac{d}{D}\right)^3\right] \tag{62}$$

where d/D is the ratio of the glass sphere diameter to the test cylinder diameter. The wall correction factor was chosen to be $[1 + 1/2(d/D)^3]$ for two reasons; first, because it approaches unity as d/D approaches zero; and second, because porosity is a spatially-related quantity (hence the cube of d/D). The factor 1/2 was selected by trial and error to yield optimum results. Correlations that include the wall correction will be identified by the symbol ε_w.

The entire correlation procedure described above was repeated incorporating equation (62) with the following results:

$$Nu\,Pr^{0.124} = 0.653\,Ra^{0.649} + 9.97 \times 10^6\,Ge\,\text{sech}\,Ra \quad \text{for } \varepsilon_w,\ j = 0.5 \text{ and } 0.001 < (Re)_{max} \leqslant 3, \tag{63}$$

$$Nu\,Pr^{0.0877} = 0.618\,Ra^{0.698} + 8.54 \times 10^6\,Ge\,\text{sech}\,Ra \quad \text{for } \varepsilon_w,\ j = 0.32 \text{ and } 0.001 < (Re)_{max} \leqslant 3, \tag{64}$$

$$Nu\,Pr^{0.124} = 1.65\,Ra^{0.319}\left(\frac{C_1 D}{C_2}\right)^{0.0585} \quad \text{for } \varepsilon_w,\ j = 0.5 \text{ and } 3 < (Re)_{max} \leqslant 100, \tag{65}$$

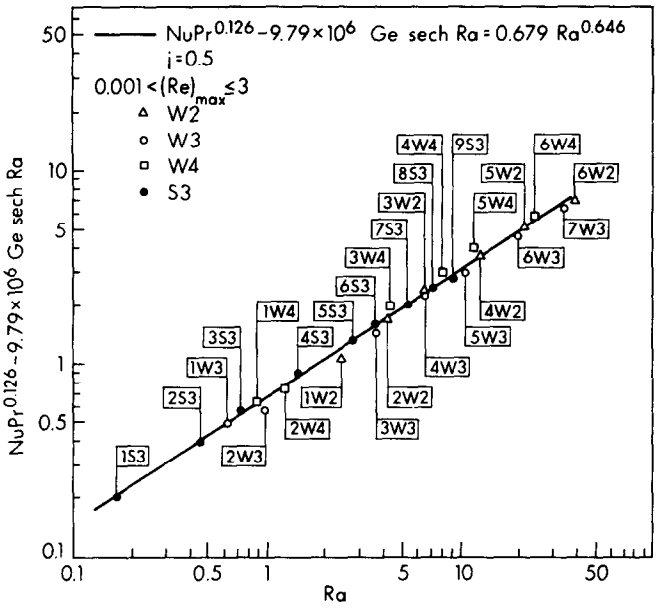

FIG. 9. Graph of equation (63) and relevant data.

$$Nu\,Pr^{0.0877} = 0.766\,Ra^{0.374}\left(\frac{C_1 D}{C_2}\right)^{0.173}$$

for ε_w, $j = 0.32$ and $3 < (Re)_{max} \leqslant 100$. (66)

DISCUSSION OF CORRELATIONS: ERRORS

The errors listed in Table 4 for the Darcy regime are more than twice what can be attributed to errors in the measurements of heat flux and temperature. It is believed that the major source of the unaccounted-for error is uncertainty with regard to the magnitude of ε. In order to demonstrate the sensitivity of the heat transfer process to the magnitude of ε, plots of K, C_1 and C_2 are presented in Fig. 10 for the 3-mm glass spheres. These plots show that, corresponding to a 1% change in ε,* the value of K changes by 4%. Now, a 4% change in K produces a 2.6% change in Nu. Thus, Nu is very sensitive to the value of ε in the Darcy regime. However, Nu is considerably less sensitive to changes in ε in the Forchheimer regime; here, a 1% change in ε produces a 1% change in Nu. This is why the errors for the Forchheimer regime listed in Table 4 are substantially less than those for the Darcy regime.

It is not likely that the value of ε can be determined experimentally with an accuracy greater than 1%, the reason for this being that the packing of the matrices of the porous media is a *stochastic* process, and is, therefore, a product of 'chance'. Even if the overall

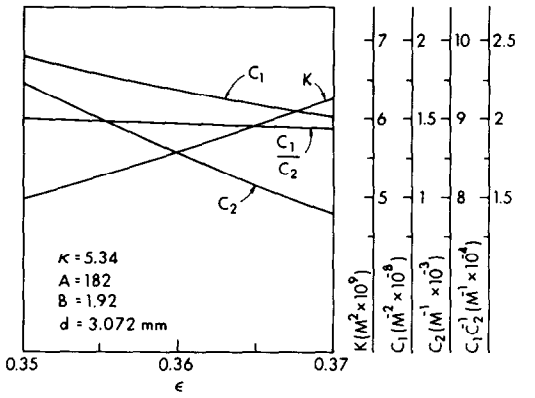

FIG. 10. Graphs of κ, C_1, C_2 and C_1/C_2 as functions of ε.

average value of ε is determined with great accuracy, it is likely that the porous medium will contain local variations in ε that are impossible to detect. Thus, it appears difficult to acquire data and correlations that would incur errors appreciably less than those listed in Table 4.

Equations (64) and (66), which contain the wall correction factor, are recommended above all others—the others have been reported primarily for development and comparison purposes. Equations (64) and (66) are considered superior not only because they exhibit the minimum errors (see Table 4) but also because they contain the wall correction factor $[1 + 1/2(d/D)^3]$ which, it is expected, renders them applicable at somewhat higher values of the ratio d/D (say, 10 or 15% higher) than the maximum ($d/D = 0.35$)

*$\varepsilon = 0.36$ for all three media employed in this study—see Table 1.

employed in the present experiments. An expanded experimental investigation of the role of d/D will be undertaken in the near future.

CONCLUDING REMARKS

The kind of flow that occurs at any point in a porous medium depends upon the Reynolds number. For natural convection in an infinite medium the Reynolds number *always* approaches zero with increasing distance from the heated surface. Therefore, the Reynolds number near a heated surface may be sufficiently high to cause Forchheimer flow, but somewhat further from this surface it will have diminished sufficiently in magnitude to incur Darcy flow, and at a still greater distance from the surface it will have diminished to the point where pre-Darcy flow occurs. These observations provide an explanation for the experimentally observed fact that the relatively small porous medium reservoir utilized in the present investigation adequately simulates an infinite medium; the reason being, of course, that the local Reynolds number drops off rapidly with increasing distance from the test specimen and the pre-Darcy regime of flow is soon encountered, which is tantamount to encountering a 'zero velocity' or 'no-slip' boundary. The extension of the medium beyond this no-slip boundary is superfluous with respect to the simulation of an infinite medium.

In view of the preceding remarks one might well question the logic behind the correlation equations presented above for Darcy and Forchheimer flow, for these equations obviously do not account for their respective preceding kinds of flow. The answer to this question is that these equations are correlation for the *Nusselt number*, which is determined by the flow adjacent to the heat transfer surface, *where the 'highest' type of flow always occurs.* However, a complete solution to the problem, including the entire velocity and temperature fields, would require, in general, the simultaneous consideration of several kinds of flow.

Acknowledgment—Robert T. Phan performed all the computer-aided calculations required for the analysis of the data. His expert assistance is much appreciated. This work was supported by NSF Grant No. MEA83-12095.

REFERENCES

1. H. C. Hardee, Boundary layer solutions for natural convection in porous media, Sandia Laboratories Report No. SAND 76-0075 (1976).
2. J. H. Merkin, Free convection boundary layers on axisymmetric and two-dimensional bodies of arbitrary shape in saturated porous medium, *Int. J. Heat Mass Transfer* **22,** 1461–1462 (1979).
3. P. Cheng, ME 627 class notes, University of Hawaii (1980).
4. O. A. Plumb and J. C. Huenefeld, Non-Darcy natural convection from heated surfaces in saturated porous media, *Int. J. Heat Mass Transfer* **24,** 765–768 (1981).
5. A. Bejan and D. Poulikakos, The non-Darcy regime for vertical boundary layer natural convection in a porous medium, *Int. J. Heat Mass Transfer* **27,** 717–722 (1984).
6. P. Cheng and W. J. Minkowycz, Free convection about a vertical flat plate embedded in a porous medium with application to heat transfer from a dike, *J. geophys. Res.* **82,** 2040–2044 (1977).
7. J. Bear, *Dynamics of Fluids in Porous Media.* American Elsevier, New York (1972).
8. R. M. Fand, E. W. Morris and M. Lum, Natural convection heat transfer from horizontal cylinders to air, water and silicone oils for Rayleigh numbers between 3×10^2 and 2×10^7, *Int. J. Heat Mass Transfer* **20,** 11, 1173–1184 (1977).
9. B. Y. K. Kim, The resistance to flow in simple and complex porous media whose matrices are composed of spheres. M.S. thesis in Mechanical Engineering, University of Hawaii, supervised by R. M. Fand (1985).
10. R. T. Phan, The thermophysical properties of a porous medium composed of a matrix of glass balls saturated with water. B.S. honors thesis, University of Hawaii, supervised by R. M. Fand (1983).
11. E. M. Sparrow and D. R. Pfeil, Enhancement of natural convection heat transfer from a horizontal cylinder due to vertical shrouding surfaces, *J. Heat Transfer* **106,** 124–130 (1984).
12. R. M. Fand and J. Brucker, A correlation for heat transfer by natural convection from horizontal cylinders that accounts for viscous dissipation, *Int. J. Heat Mass Transfer* **26,** 709–726 (1983).
13. A. Bejan, *Convection Heat Transfer.* John Wiley, New York (1984).

CONVECTION THERMIQUE NATURELLE A PARTIR D'UN CYLINDRE HORIZONTAL NOYE DANS UN MILIEU POREUX

Résumé—On présente les résultats d'une recherche expérimentale sur la convection thermique naturelle à partir d'un cylindre horizontal noyé dans un milieu poreux réalisé par des sphères de verre et saturé d'eau ou d'huile silicone. On montre que le domaine global du nombre de Rayleigh Ra peut être divisé en deux régions, appelées "basse" et "haute", dans chacune desquelles le nombre de Nusselt se comporte différemment. On montre que la région basse correspond à l'écoulement de Darcy, et Ra haute à l'écoulement de Forchheimer. On présente des équations pour Nu au régime de Darcy qui tiennent compte de la dissipation visqueuse et d'autres pour le régime de Forchheimer. La variation des propriétés avec la température et l'effet de paroi sur la porosité (et par conséquent sur le transfert thermique) sont considérés. On donne une information sur la perte de charge de l'écoulement dans le milieu poreux, en relation avec le transfert de chaleur.

WÄRMEÜBERGANG BEI NATÜRLICHER KONVEKTION AN EINEM HORIZONTALEN ZYLINDER IN EINEM PORÖSEN MEDIUM

Zusammenfassung—Diese Abhandlung zeigt Ergebnisse einer experimentellen Untersuchung des Wärmeübergangs bei natürlicher Konvektion an einem horizontalen Zylinder, der in einer Zufallsschüttung von Glaskugeln liegt, welche mit Wasser oder mit Silikonöl gesättigt ist. Der gesamte Wertebereich der Rayleighzahlen, Ra, wird in zwei Teilbereiche untergliedert (oberer und unterer Bereich), in denen sich die Nusseltzahl, *Nu*, unterschiedlich verhält. Es wird demonstriert, daß der untere Rayleighzahlbereich mit der Darcy-Strömung und der obere Bereich mit der Forchheimer-Strömung beschrieben werden kann. Es werden Korrelationsgleichungen für *Nu* im Darcybereich angegeben, welche die Energiedissipation berücksichtigen, und andere für den Forchheimerbereich, welche den ersten und zweiten Forchheimerkoeffizienten beeinhalten. Die Änderung der Stoffeigenschaften mit der Temperatur und der Randeinfluß auf die Porosität (und damit auf den Wärmeübergang) wird betrachtet. Die Abhandlung enthält ebenfalls Informationen bezüglich des Strömungswiderstandes in porösen Medien, die beim Studium der Wärmetransportvirgänge beobachtet wurden.

ПЕРЕНОС ТЕПЛА ЕСТЕСТВЕННОЙ КОНВЕКЦИЕЙ ОТ ГОРИЗОНТАЛЬНОГО ЦИЛИНДРА, РАСПОЛОЖЕННОГО В ПОРИСТОЙ СРЕДЕ

Аннотация—Представлены результаты экспериментального исследования теплопереноса естественной конвекцией от горизонтального цилиндра, расположенного в пористой среде, состоящей из хаотически распределенных стеклянных шариков, погруженных в воду или силиконовое масло. Показано, что весь диапазон значений числа Рэлея Ra можно разбить на две подобласти (малых и больших значений), в которых число Нуссельта ведет себя по-разному. При этом область малых значений числа Ra соответствует течению Дарси, а высоких–Форчхеймера. Представлены зависимости для числа *Nu* в режиме Дарси, которые учитывают вязкую диссипацию, и в режиме Форчхеймера, содержащие первый и второй коэффициенты Форчхеймера.. Принимается во внимание влияние зависимости теплофизических свойств от температуры и условий на стенке на теплоперенос. Представлены данные о гидродинамическом сопротивлении в пористых средах, полученные при исследовании процесса теплопереноса.